Ultra high frequency geomagnetic radiation from extensive air showers

Jaime Alvarez-Muñiz, Washington R. Carvalho, Jr., Andrés Romero-Wolf, Matías Tueros, and Enrique Zas

Citation: AIP Conference Proceedings **1535**, 143 (2013); doi: 10.1063/1.4807537
View online: http://dx.doi.org/10.1063/1.4807537
View Table of Contents: http://scitation.aip.org/content/aip/proceeding/aipcp/1535?ver=pdfcov
Published by the AIP Publishing

Ultra High Frequency Geomagnetic Radiation from Extensive Air Showers

Jaime Alvarez-Muñiz*, Washington R. Carvalho Jr.*, Andrés Romero-Wolf†, Matías Tueros* and Enrique Zas*

*Depto. de Física de Partículas & Instituto Galego de Física de Altas Enerxías, Universidade de Santiago de Compostela, 15782 Santiago de Compostela, Spain
†Jet Propulsion Laboratory, California Institute of Technology, 4800 Oak Grove Drive, Pasadena, California 91109, USA

Abstract. Using the ZHAireS Monte Carlo code, we show that the Fourier-spectrum of the radio emission of inclined air showers can have a sizable intensity up to the GHz frequency range. At these frequencies only a significantly reduced volume of the shower around the axis contributes coherently to the signal observed on the ground, which is mainly due to the geomagnetic and charge excess mechanisms. At ground level, the maximum emission at high frequencies is concentrated in a ring-like elliptical region defined by the intersection with the ground of a Cherenkov cone with its vertex at shower maximum. The frequency-spectrum of inclined showers, when observed at positions close to the ring-like maximum emission region, is in broad agreement with the pulses detected by the ANITA experiment, making the interpretation that they are due to ultra-high energy cosmic ray atmospheric showers consistent with our simulations. These results are also relevant for ground-based radio experiments aiming at detecting molecular bremsstrahlung radiation in the GHz range - an entirelly different emission mechanism which is not included in ZHAireS simulations - since they present an important background for such experiments.

Keywords: Radio, microwave, Neutrino, muon, pion, and other elementary particles, cosmic rays, Radiation detectors
PACS: 95.85.Bh, 95.85.Ry, 29.40.-n

1. INTRODUCTION

Experiments such as AERA [1] and EASIER [2], in the context of the Pierre Auger Collaboration, LOPES [3] in the context of KASCADE, and LOFAR [4] are regularly detecting radio pulses from ultra-high-energy cosmic rays (UHECRs). These experiments typically operate in the $\sim$ 30-80 MHz range, since the emission, believed to be mainly produced by the geomagnetic [5, 6, 7, 8] and charge excess [9, 10] mechanisms, is expected to be at least partially coherent at these frequencies. There are also efforts to detect GHz emission from extensive air showers (EAS) claimed to originate from a different and yet unconfirmed mechanism: molecular bremsstrahlung [11], such as AMBER [11], MIDAS [12, 13, 14], CROME [15] and EASIER [2].

Several events in the 300-900 MHz frequency-range were serendipitously observed with the ANITA balloon-borne antenna array flown over Antarctica. These events have been claimed to be consistent with emission from EAS with energies between $10^{18} - 5 \times 10^{19}$ eV [16]. Other experiments have also recently observed GHz radiation associated with EAS [15, 17] albeit at higher frequencies, typically above 3 GHz. These results motivate a careful study of the radio emission induced by UHECR showers paying particular attention to the UHF band in the 300 MHz - 3 GHz range.

In this work we characterize the features of the UHF emission from EAS using ZHAireS [18], a full Monte Carlo simulation of the air shower and its associated radio emission. The simulation is based on the AIRES shower code [19], and the emission is calculated using a well established algorithm [20] obtained from first principles [21, 22, 23]. The electric field due to each individual charged particle track produced in the shower simulation is calculated, accounting for any interference effects between tracks and the variation of the refractive index n with altitude. The algorithm does not assume any specific emission mechanism and correctly reproduces the radiation induced by the shower excess charge and the geomagnetically induced charged particle separation[24].

2. CHARACTERIZATION OF RADIO EMISSION IN THE UHF BAND

We have simulated the UHF emission of inclined showers, since they strengthen the conditions for coherent emission from different stages of shower evolution[25]. In addition it is inclined showers that have been observed in the GHz regime by ANITA. We have simulated EAS over Antarctica (altitude $\sim$ 2800 m a.s.l.) with zenithal angles between $\theta_z = 50^\circ$ and $\theta_z = 80^\circ$, obtaining radiation patterns on the ground along the East-West (E-W) and North-South (N-S) lines intersecting the impact

5th International Workshop on Acoustic and Radio EeV Neutrino Detection Activities
AIP Conf. Proc. 1535, 143-147 (2013); doi: 10.1063/1.4807537

point of the shower, as shown in Fig. 1. A 55 μT magnetic field with a declination of 0° and an inclination of -72.42° has been assumed.

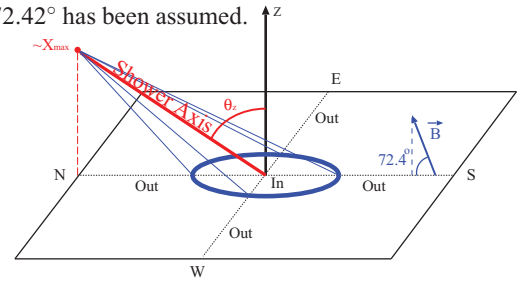

Figure 1. Shower geometry: θ_z is the zenithal angle of the shower coming from the North. Antennas are placed along the E-W and N-S lines (dotted lines). The magnetic field $\vec{B}$ used has a declination of 0° and an inclination of -72.42°. Also drawn is the Cherenkov cone centered at $X_{\max}$ and the ellipse defined by its intersection with the ground, where the UHF signal is maximum.

Strong pulses on the nano-second scale are predicted by our simulations for antennas that view the depth of maximum shower development ($X_{\max}$) at angles very close to the Cherenkov angle, i.e. antennas placed on the elliptical "ring" shown in Fig. 1. This ring is defined by the intersection of a Cherenkov cone centered at $X_{\max}$ with the ground. As the observation point moves away from this region, to the inner or outer regions of the Cherenkov cone, there is a significant broadening of the time pulse, which is equivalent to a relative lowering of the spectrum in the UHF band.

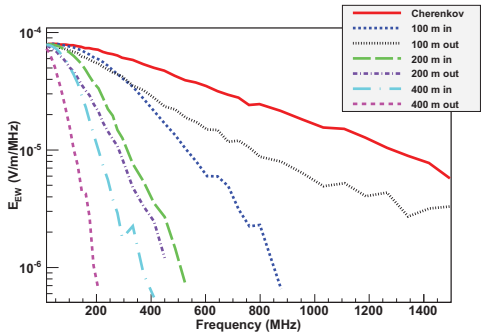

Figure 2. Frequency spectra at the ground for a 10^{19} eV proton shower with a zenith angle of $\theta_z = 80°$ coming from the North and for antennas along the W-E line at several distances from the Cherenkov ring, either on the inside or outside of the Cherenkov cone (see Fig. 1).

In Fig. 2 we show the frequency spectra for antennas lying on the ground along the W-E axis. The label "Cherenkov" refers to the antenna that lays on the elliptical ring shown in Fig. 1, while the numerical labels refer to the distance from the ring to the antenna, either towards the shower axis (in) or away from it (out). The spectra clearly become steeper as the observation points get further away from the Cherenkov ring.

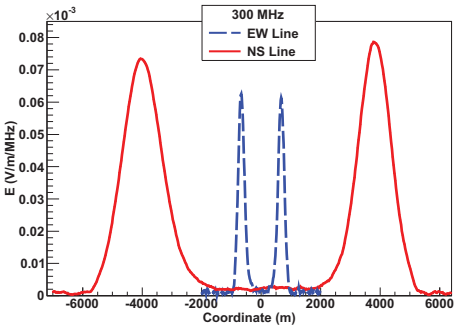

Figure 3. Fourier component (EW polarisation only) at 300 MHz as a function of distance to the shower core for a 10^{19} eV proton shower coming from the North with $\theta_z = 80°$. The antennas were placed along the N-S and E-W lines shown in Fig. 1. Negative coordinates are South (West) of the core for antennas along the N-S (E-W) line.

In Fig. 3 we show the spectral component of the electric field at 300 MHz as a function of distance to the shower core for antennas along the S-N and W-E axes. The projection of the Cherenkov cone on the ground is an ellipse with its major axis along the N-S direction as expected.

In Fig. 4 we show the spectral components of the electric field at 300 MHz for a 10^{19} eV proton shower with three different zenith angles. The scaling of the minor axis of the ring with $\sec\theta_z$ is illustrated. The axes and area of the ring increase as the zenith angle rises because the shower maximum is more distant from the ground. This increase dominates the drop induced by the decrease of the opening angle of the Cherenkov cone (i.e. the Cherenkov angle) as the refractive index n decreases with altitude.

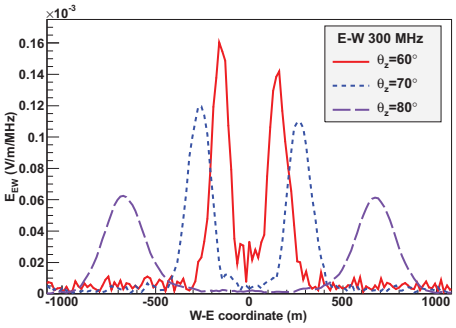

Figure 4. Fourier component (EW polarisation) at 300 MHz as a function of the distance to the core for a 10^{19} eV proton shower coming from the North with zenithal angles $\theta_z = 60°$, 70° and 80°. The antennas were placed along the E-W line shown in Fig. 1 (negative coordinates are West of the core).

In Fig. 5 the Fourier components of the field as a function of distance to the core are plotted for a fixed zenith angle at different frequencies. As the frequency drops the angular width of the Cherenkov ring broadens (an effect already visible in Fig. 2), and eventually it becomes broader than the Cherenkov angle itself making a "plateau" in the radial coordinate on ground. This can be mostly appreciated in the 50 MHz frequency line shown in Fig. 5. There is evidence of this behaviour in the flattening of the lateral distribution of the signal close to the shower core in showers detected by the LOPES [26] and LOFAR experiments [4].

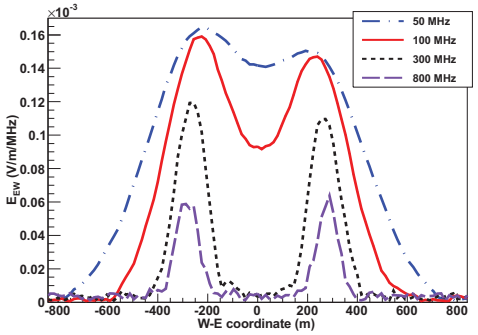

Figure 5. Fourier components (EW polarisation) of the electric field at 50, 100, 300 and 800 MHz as a function of distance to the shower core for a 10^{19} eV proton shower coming from the North with $\theta_z = 70^\circ$. The antennas were placed along the E-W line shown in Fig. 1.

3. UHECR DETECTION BY ANITA

Observations of UHECRs in the UHF band have been recently reported by the ANITA collaboration [16]. Most of these events are "reflected" events, meaning that the radiation from the shower is reflected by the Antarctic ice sheet towards the ANITA payload. The ANITA observations exhibit power spectra (i.e. electric field squared) falling exponentially with frequency as $\exp(-\nu/\nu_0)$ between 300-900 MHz, with an average exponential constant $\nu_0 \sim 190$ MHz for reflected events. The results shown in Fig. 2 for the electric field amplitude, when squared, fit well to an exponential fall-off in the UHF band with an exponential constant of $\nu_0 \sim 263$ MHz for an antenna located precisely in the Cherenkov ring, decreasing to $\nu_0 \sim 169$ MHz (84 MHz) for the antenna 100 m away towards the outside (inside) of the Cherenkov ring. The interpretation that the radiation detected with the ANITA instrument was due to extensive air showers induced by UHECRs [16], is consistent with our simulations. The geometry must be such that the ANITA antennas are pointing in the direction of the reflected radiation coming from regions close to the Cherenkov ring on the ground. The ability of ANITA to observe events reflected from regions away from the Cherenkov ring is trigger-limited. The ANITA trigger requires coincidences between several frequency bands [27], which favors triggers on events with flatter frequency spectra, such as those expected near the Cherenkov ring.

Although we have only discussed the features of the spectrum on ground, we expect the reflection on the ice sheet and the larger distance from the shower to the ANITA payload to reduce the strength of the spectrum but not to modify significantly the spectral features.

4. TIME DELAY INTERPRETATION

We investigated which regions of the shower emit *coherently* at a given frequency by calculating, for a given observer, the delays between the arrival time of the emission originating from different positions within the shower with respect to the arrival time of the earliest signal. This originates from the point (P_0) at the shower axis which is seen by the oberver at the Cherenkov angle. As we move away from P_0, time delays are introduced. In order to contribute coherently at a given frequency the magnitude of the delays must be below a fraction of the period T of that frequency (here taken to be $T/2$). If we move longitudinally, i.e. along the shower axis, the angle of the line of sight to the observer changes, introducing time delays w.r.t. P_0, which is seen at the Cherenkov angle. If we move laterally, i.e. away from the shower axis, the main contribution to the delays is the fact that the shower front lags behind w.r.t. an idealized plane moving at the speed of light due to its curvature. Near the shower axis, these curvature time delays are approximately proportional to the radius r with a constant ~ 0.2 ns/m, as can be obtained in simulations with AIRES and is measured in experiments [28].

In Fig. 6 we show the total delays as a function of the position in the shower from which the radio emission originates for a 10^{19} eV shower with 70° of zenith angle coming from the North, with the observer south of the core on the ground, on top of the Cherenkov ring (see Fig. 1). r is the distance to the shower axis (in the vertical plane that contains the axis) and L is the longitudinal distance to $X_{\max}$ along the shower axis. All time shifts were calculated analytically in terms of the relative position of the radiating charges and the observer, taking into account the index of refraction at the emission point and the expected delay of the shower front due to its curvature.

It can be appreciated that for the bulk of the shower - contained within the Moliére radius ($\sim 250 - 300$ m at the depth of shower maximum) - the time delays are below ~ 100 ns so that for this geometry and for frequencies well below 10 MHz the emission from all the shower is coherent.

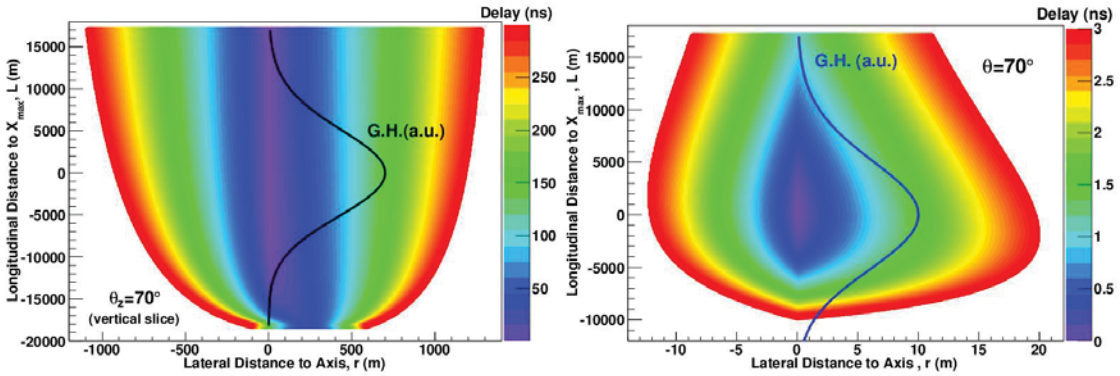

Figure 6. Time delays between the arrival time of the emission originating fromdifferent positions within the shower - measured in the longitudinal L and lateral r directions - with respect to the arrival of the earliest signal. The delays were calculated for the geometry of a proton shower of energy 10^{19} eV coming from the North, with a zenith angle of $\theta_z = 70^\circ$ and for an observer on the ground, south of the core and at the Cherenkov ring. The observer sees $X_{\max}$ ($r = L = 0$ m), which is P_0 for this geometry, at the Cherenkov angle (see text). The longitudinal shower profile is superimposed (solid line). Right panel: Blow-up of the central region shown on the left panel with delays relevant for the UHF band.

In the right panel of Fig. 6 we show a blow-up of the central region of the shower to indicate the delay structure in the region relevant for UHF emission. The time delays for different points along the shower axis are smaller than 1 ns for a large fraction of the shower development, starting more than ~ 15 km above shower maximum and finishing ~ 6 km below it. However, the delays in the lateral direction are dominated by the intrinsic delay of the shower front, and particles that are more than $\sim 5-6$ m away from shower axis have delays that exceed the 1 ns scale. As a result the "coherent volume", i.e. the region contributing in phase, is a long and thin volume along shower axis. This is confirmed in full Monte Carlo simulations in which we obtained the Fourier spectrum for this same geometry and compared it to that obtained accounting only for particles occupying a fractional volume of the shower around the axis. For frequencies above ~ 300 MHz the spectrum of the whole shower is mainly due to particles with $r < 10-20$ m, as shown in Fig. 7.

This time-delay approach is also helpful in the interpretation of the lateral distribution of the field at ground level. For an observer at the Cherenkov ring, the volume contributing coherently occupies a region of the shower around $X_{\max}$, where the number of particles is largest (see Fig. 6), so this observer has the maximum signal. If the observer moves away from the Cherenkov ring, the volume contributing coherently moves upwards or downwards w.r.t. $X_{\max}$, into regions of the shower with less particles, reducing the electric field. This leads to the lateral distributions shown in Fig. 3 through Fig. 5. This indicates that the measurement of the spectral components in the UHF band at different distances to the impact point can be related to the longitudinal development of the shower.

The time-delay approach allows the interpretation of the frequency spectrum not only in the UHF band, but at all frequencies and all shower zenith angles, including vertical showers (see [29]).

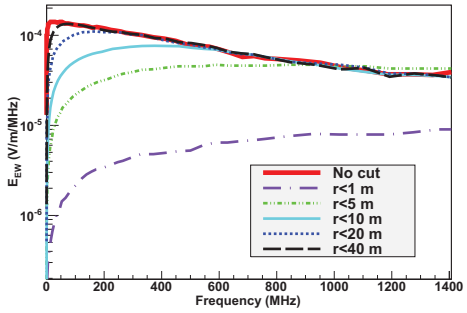

Figure 7. Frequency spectra at ground for the antenna that views $X_{\max}$ at the Cherenkov angle for a 10^{19} eV proton shower with a zenith angle of $\theta_z = 80^\circ$ coming from North. The spectrum was obtained for the whole shower ("No cut") and for particles with distances to the core $r < r_{\rm cut}$ for values of $r_{\rm cut}$ =1, 5, 10, 20 and 40 m.

5. SUMMARY AND OUTLOOK

We have shown that the radio signal emitted from UHECR air showers has a sizable intensity well into the GHz frequency range. The UHF components are more important for inclined showers than for vertical ones. On the ground, the UHF signal is maximum at an elliptical ring defined by the intersection of the Cherenkov cone centerd at $X_{\max}$ with the ground. As the observer moves

away from the ring, the UHF signal diminishes. This decrease gets more pronounced as the frequency is increased. The size of this Cherenkov ring depends on geometry, increasing with zenith angle, and reaching hundreds of meters for showers of 70°.

We have also shown that the frequency spectrum of the pulses extend well into the GHz regime and falls with an exponential slope with a constant that is largest at the Cherenkov angle, diminishing as the observer moves away from the Cherenkov ring. Predictions for short radio pulses at ns scales follow from the spectra obtained for inclined showers. In the case of more vertical showers, although the UHF components exist, the pulses are dominated by the lower frequency components and thus give typically a much broader pulse in time. These results also provide an important background for experiments that are trying to measure molecular bremsstrahlung radiation from extensive air showers, and should be carefully considered in order to properly interpret measurements made in the UHF band.

The lateral distribution for the low frequency components of the radio pulses, typically below $\sim$100 MHz, has been shown to display a rather flat behavior with distance to the shower core until the position of the Cherenkov ring is reached [18, 30]. This behavior is consistent with observations made at LOPES [26] and LOFAR [4] and should be taken into account when trying to obtain the shower geometry and properties from the radio pulse measurements [1]. Our results also suggest that the lateral distribution of signals on the ground contain information about the longitudinal development of the shower.

Our results for the power spectra obtained close to the Cherenkov direction are consistent with the spectra measured at ANITA and attributed to radio pulses from UHECR [16]. The results of the simulations made in this work further support this hypothesis. An event-by-event comparison of ANITA pulses that includes a simulation of the experiment would further strengthen this claim.

ACKNOWLEDGMENTS

J.A-M, W.R.C., M.T. and E.Z. thank Xunta de Galicia (INCITE09 206 336 PR) and Consellería de Educación (Grupos de Referencia Competitivos – Consolider Xunta de Galicia 2006/51); Ministerio de Educación, Cultura y Deporte (FPA 2010-18410 and Consolider CPAN - Ingenio 2010); ASPERA - AugerNext (PRI-PIMASP-2011-1154) and Feder Funds, Spain. We thank CESGA (Centro de SuperComputación de Galicia) for computing resources. Part of this research was carried out at the Jet Propulsion Laboratory, California Institute of Technology, under a contract with the National Aeronautics and Space Administration.

REFERENCES

1. S. Fliescher, and for the Pierre Auger Collaboration, *Nucl. Instrum. Meth. A* **662**, S124 (2012).
2. P. Allison, and for the Pierre Auger Collaboration, *Proceedings of the* 32nd *ICRC* (2011).
3. A. Nigl, et al., *Astron. & Astrophys.* **488**, 807 (2008).
4. A. Corstanje, et al., *Proceedings of the* 32nd *ICRC* (2011).
5. F. Kahn, and I. Lerche, *Proc. Roy. Soc. A* **289**, 206 (1966).
6. H. Allan, R. Clay, and J. Jones, *Nature* **227**, 1116 (1970).
7. H. Falcke, et al., *Nature* **435**, 313 (2005).
8. D. Ardouin, et al., *Astropart. Phys.* **31**, 313 (2009).
9. G. Askar'yan, *Soviet Physics JETP* **14,2**, 441–443 (1962).
10. G. Askar'yan, *Soviet Physics JETP* **48**, 998–990 (1965).
11. P. Gorham, et al., *Phys. Rev. D* **78**, 032007 (2008).
12. J. Alvarez-Muñiz, et al., *Phys. Rev. D* **86**, 051104(R) (2012).
13. J. Alvarez-Muñiz, et al. (2012), `arXiv:1208.2734[astro-ph]`.
14. P. Privitera, et al., *Nucl. Phys. B* **212-213**, 329 (2011).
15. R. Smida, et al., *Proceedings of the* 32nd *ICRC* (2011).
16. S. Hoover, and *et al.*, *Phys. Rev. Lett.* **105**, 151101 (2010).
17. P. Facal San Luis, and for the Pierre Auger Collaboration, *Proceedings of the International Symposium on Future Directions in UHECR Physics (UHECR 2012) to appear* (2012).
18. J. Alvarez-Muñiz, W. Carvalho Jr., M. Tueros, and E. Zas, *Astropart. Phys.* **35**, 325 (2012).
19. S. J. Sciutto (2002), URL `http://www.fisica.unlp.edu.ar/auger/aires/`.
20. H. R. Allan, *Progress in Elementary Particle and Cosmic Ray Physics*, North Holland, 1971.
21. F. Halzen, E. Zas, and T. Stanev, *Phys. Lett. B* **257**, 432 (1991).
22. F. Halzen, E. Zas, and T. Stanev, *Phys. Rev. D* **45**, 362 (1992).
23. J. Alvarez-Muñiz, A. Romero-Wolf, and E. Zas, *Phys. Rev. D* **81**, 123009 (2010).
24. D. Garcia-Fernandez, J. Alvarez-Muniz, W. Carvalho Jr., A. Romero-Wolf, and E. Zas (2012), `arXiv:1210.1052[astro-ph.HE]`.
25. J. Alvarez-Muniz, C. W. James, and R. J. Protheroe, *Astropart. Phys.* **32**, 100 (2009).
26. W. D. Apel, et al., *Astropart. Phys.* **32**, 294 (2010).
27. P. W. Gorham, et al., *Astropart. Phys.* **32**, 10 (2009).
28. A. Calabrese Melcarne, L. Perrone, and A. Surdo, *Proceedings of the* 31st *ICRC* (2009).
29. J. Alvarez-Muñiz, W. Carvalho Jr., A. Romero-Wolf, M. Tueros, and E. Zas, *Phys. Rev. D to appear* (2012), `arXiv:1208.0951[astro-ph.HE]`.
30. K. D. de Vries, A. M. van den Berg, O. Scholten, and K. Werner, *Phys. Rev. Lett.* **107**, 061101 (2011).